S0013-4651(98)11-028-5 CCC: $7.00 © The Electrochemical Society, Inc.

Deposition of Fluorinated Amorphous Carbon Thin Films as a Low-Dielectric-Constant Material

Sang-Soo Han, Hun Rae Kim, and Byeong-Soo Bae

Laboratory of Optical Materials and Coating, Department of Materials Science and Engineering, Korea Advanced Institute of Science and Technology, Taejon 305-701, Korea

Fluorinated amorphous carbon thin films (a-C:F) are deposited using inductively coupled plasma chemical vapor deposition with various flow-rate ratios of CH_4:CF_4 gases for ultralarge-scale integrated intermetal dielectric applications. The accurate composition of the thin films are quantitatively analyzed using elastic recoil detection–time of flight. The incorporation of fluorine is saturated at about 25 atom % by increasing the CF_4 flow rate. The dielectric constant decreases to 2.4 and the refractive index of the film is reduced to 1.35 as the CF_4 flow rate increases. Also, it is observed that the C–F bonding configuration changes from an unsaturated C–F bond to C–F_2 and C–F_3 bonds with growing CF_4 flow rate. Thus, the reduction mechanism of the dielectric constant can be obtained by variation of the C–F_X bonding configuration as well as the incorporation of fluorine.
© 1999 The Electrochemical Society. S0013-4651(98)11-028-5. All rights reserved.

Manuscript submitted November 6, 1998; revised manuscript reeived May 1, 1999.

As feature size in integrated circuits (ICs) decreases, interconnect technology has become very complicated. For advanced logic devices, circuit performance is limited by the interconnect rather than transistors. Maximizing circuit performance may be accomplished by minimizing propagation delays and optimizing interconnect line layout on the die. Propagation delays due to parasitic capacitances from interconnections are one of the main causes for compromising speed performance in advanced ICs as interconnect dimensions are scaled down. In addition, increases in die size make interconnect lengths very long, which means higher interconnect resistance, which also contributes to propagation delays due to an increase in RC (resistance-capacitance) time constant. Therefore, the use of high conductive metal and low dielectric materials are needed to reduce propagation delays. An additional advantage in reducing total capacitance is that it decreases power consumption and cross-talk noise.

Recently, the need has increased for developing new low dielectric materials to replace conventional intermetal dielectric (IMD) materials of high dielectric ($k \sim 3.9$) SiO_2.[1] There have been several investigations for producing low-dielectric-constant materials ($k <$ 3). In order to decrease the dielectric constant, fluorinated SiO_2 films have been studied by various techniques, such as atmospheric pressure chemical vapor deposition (APCVD) using fluorine-containing precursors and plasma-enhanced CVD (PECVD) using SiF_4 or C_2F_6/tetraethoxysilance (TEOS).[1-5] The decrease in dielectric constant is relatively small since the amount of fluorine that can be incorporated into SiO_2 is limited.

Another candidate material is polymer thin films, since they have low dielectric constants, below 3. Most of the studies on organic dielectric, are based on spin-on coatings followed by a curing process including $k = 2.4$–2.6 for fluorinated poly(arylenethers), $k = 2.6$–2.8 for flourinated polyimides, and $k = 2.4$ for perfluorocyclobutane (PFCB). However, as the monomer is polymerized during the curing process, the macromolecules may align parallel to the substrate, leading to anisotropic properties. Another method is to use vapor deposition. It is solvent-free and can provide a uniform coating over a large area. The vapor-deposited polymeric films are the following[6-10]: $k = 2.6$ for Parylene-N,[8] $k = 2.2$ for Parylene copolymers, $k = 2.3$ for Parylene-F,[9] and $k = 1.9$ for PTFE (polytetrafluoroethylene, Teflon-AF). In particular, PTFE is a promising material, since it may be the lowest dielectric constant material with reasonable mechanical strength.

However, polymer thin films have problems providing desired characteristics such as thermal stability, adhesion, glass transition temperature, mechanical strength, and gap-filling during integration processing in microelectronics. In particular, the gap-filling property becomes more important with decreased minimum feature size of the interconnection line. High-density plasma (HDP) CVD has been unquestionably proven the process of choice for sub-0.5 μm intermetal dielectric gap-fill.[11] Hydrogenated amorphous carbon (a-C:H) films fabricated by plasma deposition from hydrocarbon gases have high electrical resistivity and good thermal stability due to their highly cross-linked structures.[12-14] Recently, fluorinated amorphous carbon thin films deposited using HDP CVD have been investigated as a new IMD material.[15-17] However, the origin of low dielectric constant, role of fluorine, and atomic structure of the films are still obscure. In particular, the reduction of the dielectric constant for films having the same fluorine concentration was reported in a recent study,[17] but the cause was not explained.

Therefore, in this study we prepared the fluorinated amorphous carbon thin films, which have both cross-linking and PTFE-like structures, as low-dielectric-constant IMDs for ultralarge-scale integrated (ULSI) multilevel interconnections. The a-C:F thin films were deposited by remote-type inductively coupled plasma (ICP)-CVD using CF_4, CH_4 gases as the reactant gases with various deposition conditions. Then the effects of flourine content, structure, and bonding configuration on the dielectric constants and characteristics of thin films required for device processes were investigated. Also, we investigated the reduction mechanism of the low dielectric constant with relation to bonding configuration, composition, and structure of the films. In particular, we discovered the cause of the reduction of the dielectric constant for films of the same fluorine content.

Experimental

Figure 1 is a schematic diagram of the remote-type ICP-CVD (inductively coupled plasma–chemical vapor deposition) system used in this study. In this system, radio frequency (rf) coil is wound around the Al_2O_3 tube plasma chamber to couple power inductively to the plasma through a chamber dielectric wall to generate higher density plasma without an external magnetic field. The intense degree of ionization and dissociation is established in a region away from the substrate in the deposition chamber. Therefore, this remote-type ICP-CVD process allows deposition of high-quality thin film without heating and damage to the substrate. The main purpose for using the remote-type system is maximization of the F content by dissociating the CF_4 gas directly.

The fluorinated amorphous carbon thin films were deposited on p-type Si(100) substrate using CH_4/CF_4 as the reactant gases and Ar as the diluent gas. CF_4 and Ar gases were premixed in a gas-mixing box, and the gas mixture passed through the plasma chamber. CH_4 gas passes through by ejection from the gas ring located just under the plasma chamber. Thus, CF_4 gas is directly dissociated by rf power while CH_4 is indirectly dissociated. Deposition characteristics were examined with the various gas-flow-rate ratios of CF_4:CH_4. While the

S0013-4651(98)11-028-5 CCC: $7.00 © The Electrochemical Society, Inc.

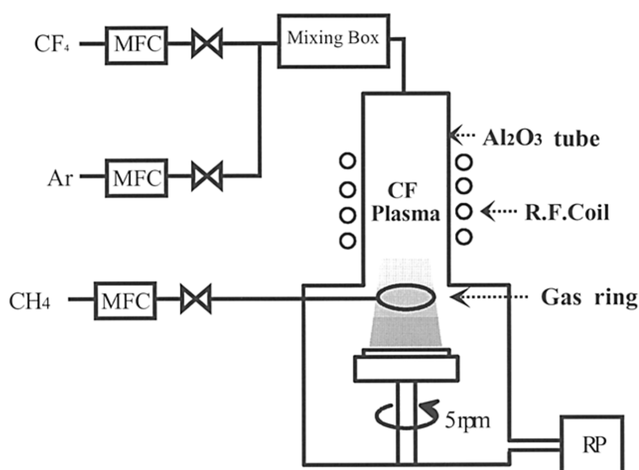

Figure 1. Schematic diagram of ICP-CVD system.

CH_4 flow rate is constant at 4 sccm, the CF_4 flow rate is increased from 4 to 40 sccm. Therefore, the gas-flow-rate ratio of CF_4 to CH_4 is 1, 2, 5, 10. Ar gas was used as the carrier gas and its flow rate adjusted to keep the total gas flow rate constant at 120 sccm. The experimental deposition conditions are listed in Table I.

The thickness and refractive index of the films were simultaneously obtained using an ellipsometer (Rudolph, Auto-EL2). The dielectric constants of the films were calculated from the capacitance-voltage (C-V) plot measured at 1 MHz in the metal-insulator semiconductor MIS structure (Al/a-C:F/Si). To make the ohmic contact between the probe and the back side of the Si substrates, Al thin film was deposited on the back side of the Si substrates by sputtering. To find the relationship between the dielectric constant and the bonding characteristics, the C-F bonding configurations in the films were analyzed using XPS (X-ray photoelectron spectroscopy, VG Escalab 200R, Al Kα radiation) and FTIR (Fourier transform infrared spectroscopy, Bruker, Equinox 55). In particular, the semiquantitative analysis was done using a multiple Gaussian peak integration method from the XPS data. The absolute quantitative analysis for all elements, including hydrogen in the films, were performed by elastic recoil detection–time-of-flight (ERD-TOF) measurement. By the inverse reaction scheme the recoil cross sections induced by below 10 MeV ^{35}Cl ion were measured. Therefore, we could obtain the energy-counts spectra by plotting with different TOFs. It was already known that the ERD-TOF technique is excellent to analyze quantitatively low-weight elements such as C, F, and H.[18]

Results and Discussion

Deposition rate.—The deposition rates of a-C:F thin films as a function of the CF_4:CH_4 flow-rate ratio are shown in Fig. 2. As the total reactant gas flow increases, the deposition rate decreases. This trend does not coincide with the deposition rate of the other films. It assumes that the etching reaction due to the excess fluorine ions also occurred simultaneously when the a-C:F film was deposited. The etching reaction of the films is enhanced by the increase of the fluorocarbon reactive species, since the excess fluorine ions react with hydrogen ions to form HF molecules. Thus, the deposition rate is reduced by raising the CF_4:CH_4 flow-rate ratio.

Compositional analysis.—Although there have been extensive studies on the a-C:F thin films, the quantitative compositional analysis is obscure. It is unreliable to analyze quantitatively the composition using conventional methods such as Auger electron spectroscopy (AES), and XPS, although the reference sample is used. In particular, the quantitative analysis of hydrogen has been impossible except for special methods such as nuclear reaction analysis (NRA). In this study, the accurate composition of a-C:F thin films was analyzed quantitatively using ERD-TOF. The ERD-TOF method includes the flight time of each element in the Rutherford backscattering spectroscopy (RBS) system,[18] and the amount of light element such as C, F, and H can be analyzed quantitatively, since each element can be counted without overlap in energy axis by separation of the flight time of each element.

Figure 3 shows the atomic ratio obtained from the ERD-TOF spectra of the a-C:F thin films with various CF_4:CH_4 flow-rate ratios. As the CF_4:CH_4 flow-rate ratio increases from 1 to 2, the carbon content decreases and the fluorine content increases to 25 atom %, but the hydrogen content is almost constant at about 5%. In this remote-type ICP-CVD system, it is revealed that low hydrogen content in the thin films can be obtained.[19] There is little change of composition in the a-C:F thin films having CF_4:CH_4 flow-rate ratios above two. Thus, the incorporation of fluorine is saturated at about 25%, although the CF_4 flow rate increases. Also, regardless of the CF_4 flow rate, the hydrogen content is about 5%, which is a relatively low value compared with other studies.[16] It is assumed that more fluorine may bond with carbon than that in the film with high hydrogen content, since the hydrogen source, CH_4, is indirectly dissociated by rf power.

AES analysis was also carried out to be certain of the composition variation dependence on the CF_4:CH_4 flow-rate ratio. Figure 4 shows the variation of the relative C/F ratio analyzed by AES. The relative C/F ratio decreases with increasing the CF_4:CH_4 flow-rate ratio to two but remains constant with higher CF_4 flow rates. This

Table I. Deposition conditions of low dielectric a-C:F films for intermetal dielectric application.

Deposition parameters	Conditions
Substrate	Silicon Doping: boron-doped p-type Direction: (100) Resistivity: 5-10 Ω cm
Base pressure	6 mTorr
Working pressure	120-200 mTorr
Substrate rotation speed	5 rpm
RF power	400 W
Deposition temperature	Room temperature
Ar flow rate	120 sccm
CH_4 flow rate	4 sccm
CF_4 flow rate	4, 8, 20, and 40 sccm
CF_4:CH_4 flow-rate ratio	1, 2, 5, 10

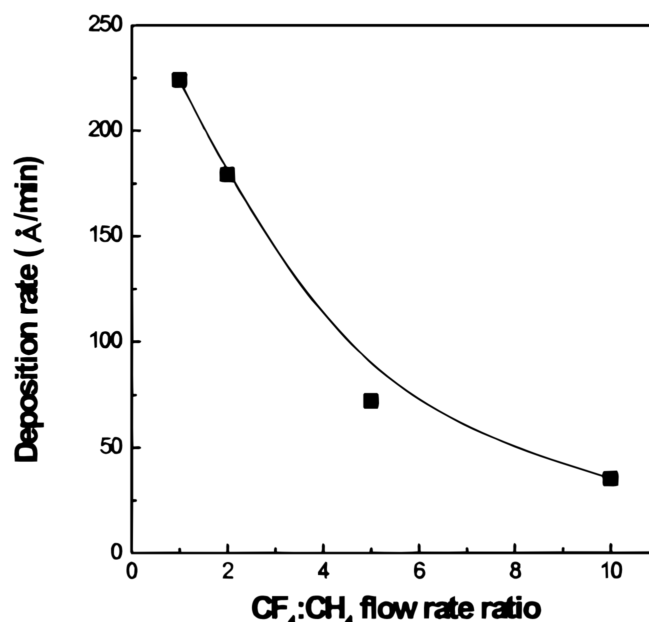

Figure 2. Deposition rate of a-C:F thin films with various CF_4:CH_4 flow rate ratios.

S0013-4651(98)11-028-5 CCC: $7.00 © The Electrochemical Society, Inc.

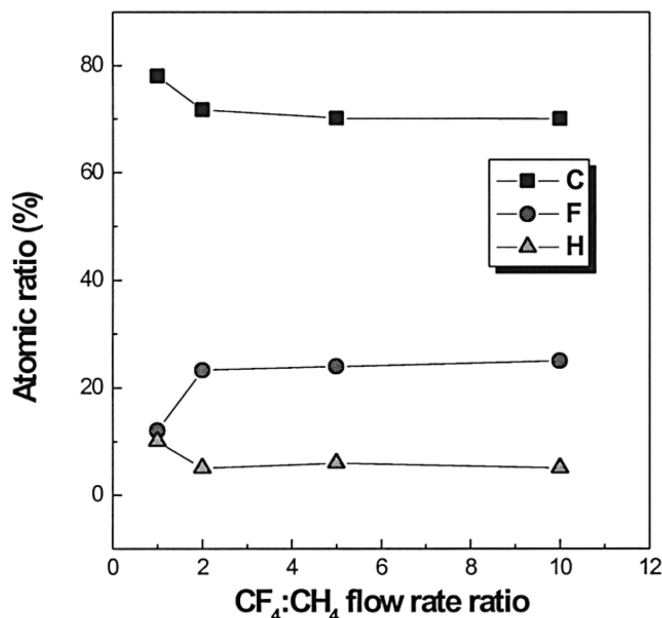

Figure 3. The atomic ratio analyzed from the ERD-TOF spectra of a-C:F thin films with various CF_4:CH_4 flow-rate ratios.

compositional variation with increasing the CF_4 flow rate agrees well with that of the ERD-TOF analysis.

Refractive index and dielectric constant.—The refractive index and the dielectric constant of the thin films depending on the CF_4:CH_4 flow-rate ratio are shown in Fig. 5. The refractive index and dielectric constant decreases down to 1.23 and 2.4, respectively, by increasing the CF_4:CH_4 flow-rate ratio. It is already known that the incorporation of fluorine with high electronegativity reduces the refractive index and the dielectric constant of the thin films. The electronegativities of the F, C, and H components of the films are 3.98, 2.55, and 2.20, respectively.[20] As the fluorine content with high electronegativity increases in the thin films, the electronic polarization (due to the shift of the center of gravity of the negative electron cloud in relation to the positive atom nucleus in an electric field) is reduced. For reference, the electronic polarizabilities of pure elements F, C, and H are 0.557, 1.76, and 0.667, respectively.[20] This relationship between electronic polarizability and electronegativity of atoms is explained as follows.

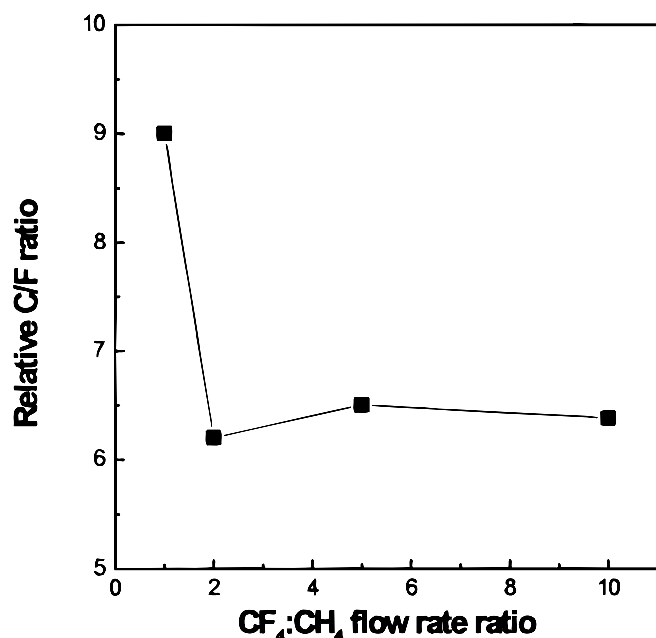

Figure 4. AES relative C/F ratio of a-C:F thin films with various CF_4:CH_4 flow-rate ratios.

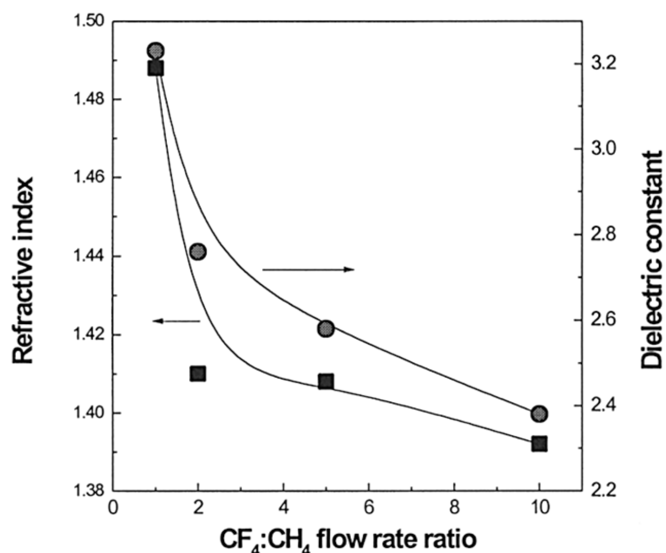

Figure 5. Dielectric constant and refractive indexes of a-C:F thin films with various CF_4:CH_4 flow-rate ratios.

When an external electric field, E, causes a slight displacement, x, of the center of an electron cloud with a charge, q, on an atom in a polymer molecule, the induced dipole moment, m, is then

$$m = qx \tag{1}$$

and electronic polarizability, α_e, is

$$\alpha_e = \frac{qx}{E} \tag{2}$$

According to the model of elastically bound electrons,[21] the charge displacement is an equation with the interaction force between electrons and the positive nucleus which we can express as electrically bound, $k'x$, then

$$k'x = qE \tag{3}$$

By substituting Eq. 3 into Eq. 2

$$\alpha_e = \frac{q^2}{k'} \tag{4}$$

Electronic polarization decreases as the force constant, k' decreases. The force constant of the atom refers to the force needed to displace the electron from the nucleus. Therefore, since the high electronegative atom strongly attracts the electron, the force constant of the atom is high. When this relationship is applied to the a-C:F films in this study, the fluorine atom has the highest k' due to the high electronegativity. Thus, the more incorporation of fluorine with increasing the CF_4 flow rate decreases electronic polarization and reduces the refractive index and the dielectric constant contributed by the electronic polarization in the thin films. The contribution of electronic polarization to the dielectric constant can be represented by the square of the refractive index, $ke = n^2$. However, the measured dielectric constants are attributed by dipolar and ionic polarizations as well as electronic polarization. Thus, the measured dielectric constants of the thin films can be divided by electronic polarization and the ionic (and bond dipole) polarization terms as shown in Fig. 6.

Bonding configuration and structural analysis.—The C–F bonding configuration in the a-C:F thin film was analyzed using FTIR

S0013-4651(98)11-028-5 CCC: $7.00 © The Electrochemical Society, Inc.

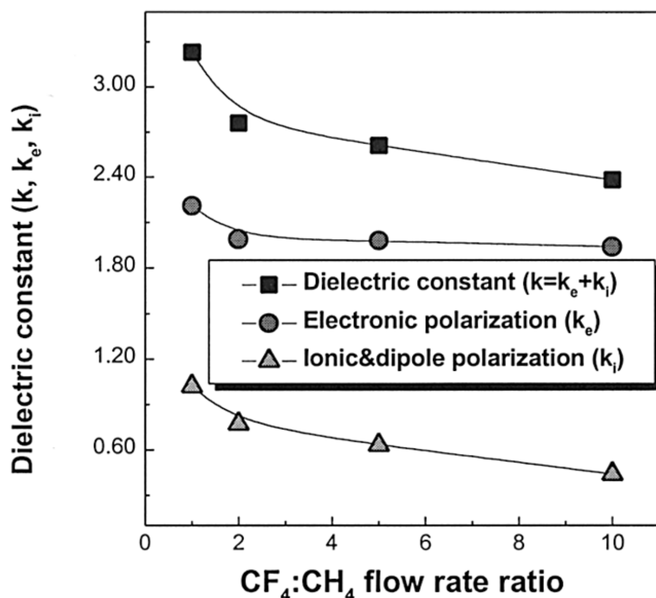

Figure 6. The variation of dielectric constants of a-C:F thin films with increasing CF_4:CH_4 flow-rate ratios.

and XPS. Figure 7 presents FTIR spectra of the thin films with various CF_4 flow rates. It is found that the main peak of the FTIR spectra shifts to a higher wavenumber by increasing the CF_4 flow rate. The peaks at 1080, 1160, and 1210 cm^{-1} represent $C–F_{sat(end\ group)}$, $C–F_{unsat(bridging\ group)}$, and $C–F_2$ and $C–F_3$ bonds, respectively. For a polyvalent atom such as carbon, the partial charge builds up when another highly electronegative substituent (fluorine) is added. This partial charge produces the extra bonding energy

$$C^{\delta+} - F^{\delta-} \qquad E = \frac{\delta^+\delta^-}{4\pi\epsilon_0 r} \qquad [5]$$

Thus, as more fluorine is bonded with a carbon, the bonding length of the C-F is shortened by extra bonding energy. It is known that the bond lengths of the CH_3F, CH_2F_2, CHF_3, and CF_4 are 139.1, 135.8, 133.2, and 132.3 pm, respectively.[22] Therefore, the ionic polarization decreases as the C–F bonding in the a-C:F films changes from the $C–F_{sat}$ to the $C–F_2$ and $C–F_3$ by increasing the CF_4 flow rate. As discussed previously, this is due to the reduction of the displacement of ions of opposite sign from their regular sites under the influence

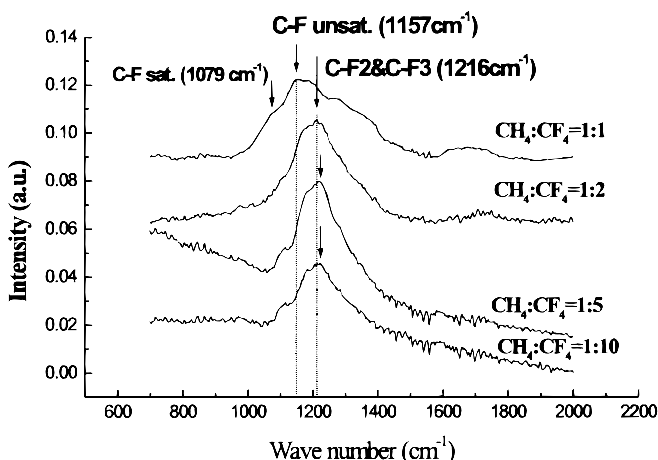

Figure 7. FTIR spectra of a-C:F thin films with various CF_4:CH_4 flow-rate ratios.

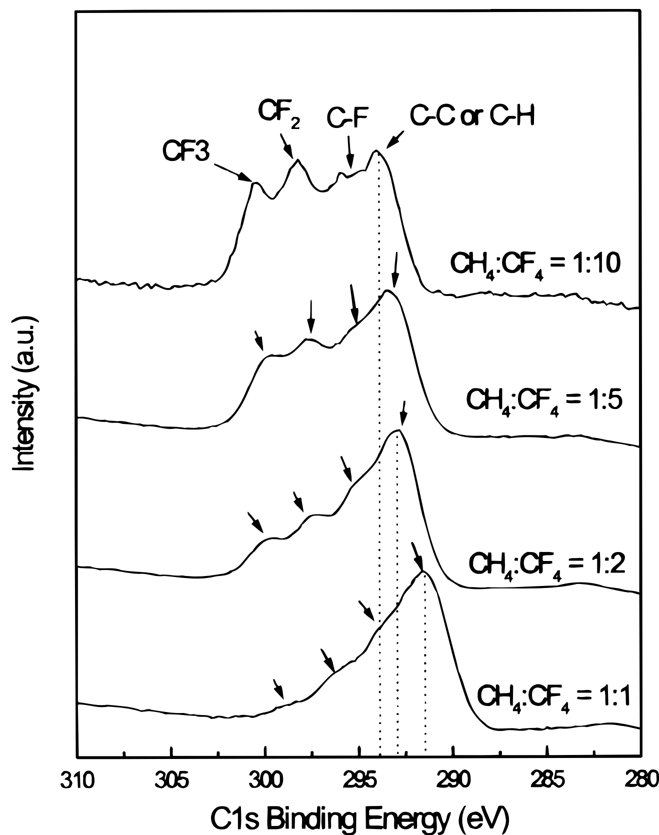

Figure 8. C 1s binding energy XPS spectra of a-C:F thin films.

of an electric field, since the bond strength between carbon and fluorine is enhanced.

To investigate the bonding configuration more quantitatively, the a-C:F thin films were analyzed using XPS. Figure 8 shows C 1s binding energy spectra of a-C:F thin films. It is definitely found that the peak shifts to higher binding energy and is broadened with increased CF_4 flow rate. The greater incorporation of fluorine with carbon is associated with higher binding energy, since more energy is required to take out the electron of the core level due to high electronegativity of fluorine. Thus, the higher binding energy peak in the XPS spectra can be assigned to more fluorine-incorporated bonding configuration, as seen in Fig. 8. Particularly, the $C–F_3$ bonding is differentiated from the $C–F_2$ bonding in the XPS spectra. It is certain that $C–F_2$ and $C–F_3$ bonding contents become more dominant as the CF_4 flow rate increases. This result is in accordance with the FTIR spectra.

In order to analyze quantitatively the content of each bonding configuration, the XPS spectra was deconvoluted to four Gaussian peaks, as shown in Fig. 9a. The integration of the deconvoluted peak can represent the concentration of each bonding configuration. Figure 9b presents the variation of the integrated area of the peaks depending on the CF_4:CH_4 flow-rate ratio. It is shown that the concentration of $C–F_2$ and $C–F_3$ bondings grows while C–F bonding and C–C or C–H bonding content is reduced. Thus, the structure of the film can be assumed from the variation of bonding configuration depending on the CF_4:CH_4 flow-rate ratio. From the ERD-TOF (Fig. 3) and XPS data (Fig. 9), the evolution of the structure can be separated into two steps, as shown in Fig. 10. Figure 10 is a schematic presentation of this model. In step 1, which is the first evolution of the structure, F content in the film increases from 12 to 25% and the $C–F_2$ and $C–F_3$ bonds increase while the C–C (or C–H) and C–F bonding configurations decrease. The number of $C–F_2$ and $C–F_3$ bonding slightly increases due to the substitution of fluorine for the hydrogen bonded with carbon. In step 2, the F content in the film is almost constant, 25%, and the $C–F_2$ and $C–F_3$ bonds abruptly increase while the C–C (or C–H) and C–F bonding configurations de-

crease. In this step, excess F ions for high-CF_4 flow rates break the cross-linking C–C bonds and then the C–C molecule structure is shortened by creation of the C–F_3 bond. As shown in Fig. 10, the increase of the C–F_2 bonding implies the film has a less cross-linked (linear) structure, but it also implies that the length of the C–C backbone chain is shortened by increasing the CF_4 flow rate, since the C-F_3 is an ending group of the C–C chain structure. Therefore, we can conclude that the increase of F content occurs dominantly in low-CF_4 flow rate, and for high-CF_4 flow rate, the evolution to less cross-linked structure with short chain occurs dominantly due to an etching reaction of excess F ions. As a result, the structure of the film evolves into less cross-linked structure with short C–C chain lengths.

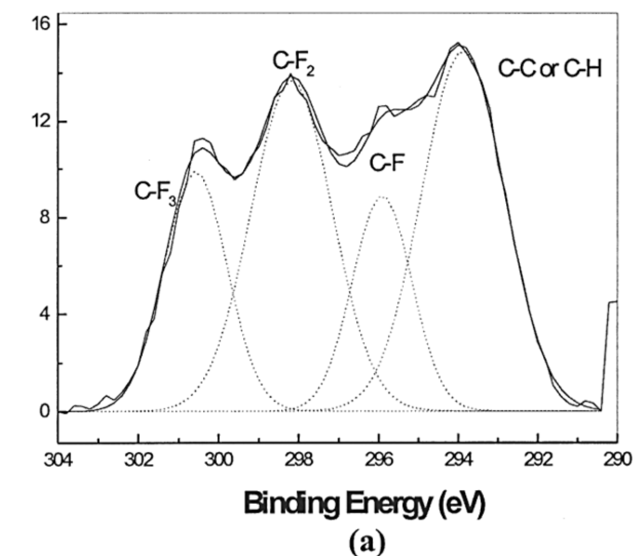

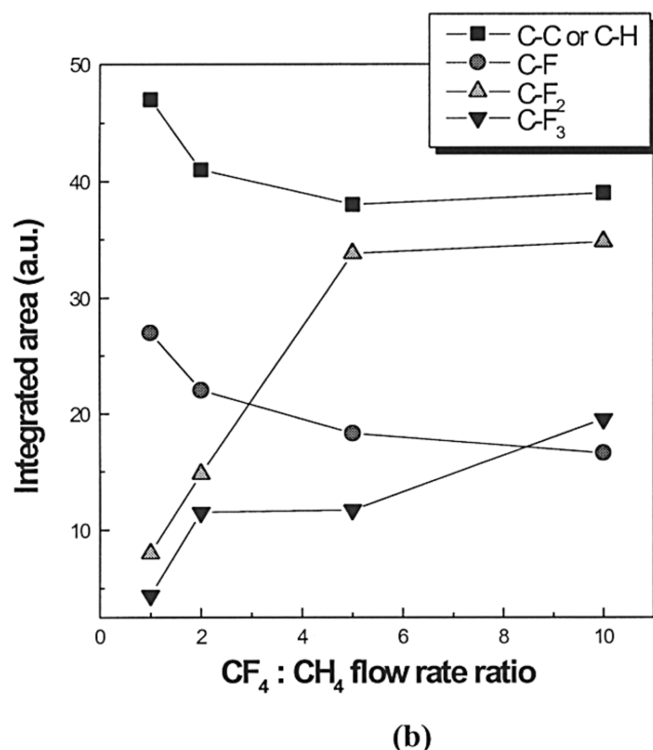

Figure 9. (a) Deconvolution of C 1s binding energy XPS spectra and (b) their multiple Gaussian integration for a-C:F thin films with various CF_4:CH_4 flow-rate ratios.

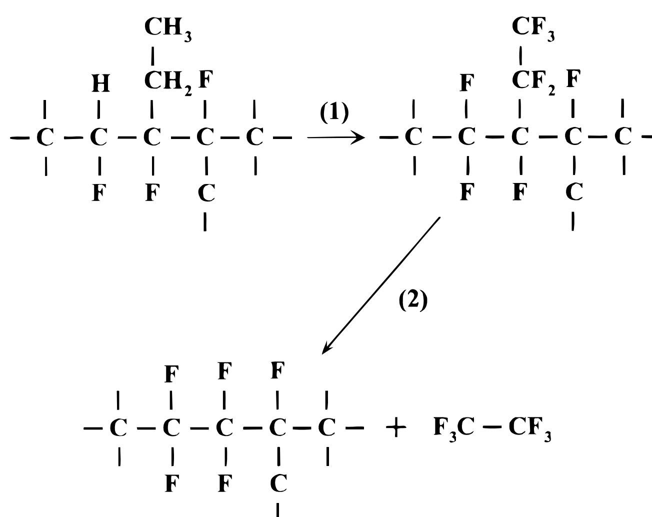

Figure 10. Structural evolution model of a-C:F thin films with increasing CF_4:CH_4 flow-rate ratios.

Figure 11 shows an atomic area density calculated from the ERD-TOF spectra and thickness of the a-C:F thin film with various CF_4:CH_4 flow rate ratios. It is found that the atomic area density is reduced by increasing the CF_4 flow rate. This result coincides with the structure of the film proposed using the FTIR and XPS data, since the increase in the end group by C–F_3 bonding by increasing the CF_4 flow-rate ratio prevents the polymer structure from cross-linking and entangling, and the density of the film is lowered.

Reduction mechanism of the dielectric constant.—The factors effecting the dielectric constant are polarization and density of the film. Total polarization consists of electronic, ionic, and orientation polarization, and the density of the film is associated with the structure. In this study, the reduction mechanism of the dielectric constant of a-C:F thin films with increasing the CF_4:CH_4 flow-rate ratio is divided into two steps in terms of polarization. This polarization is related to the composition, bonding configuration, and structure of the film.

In step 1, as the CF_4:CH_4 flow-rate ratio increases, F content increases from 12 to 25 atom %, while the C–F bonding configuration

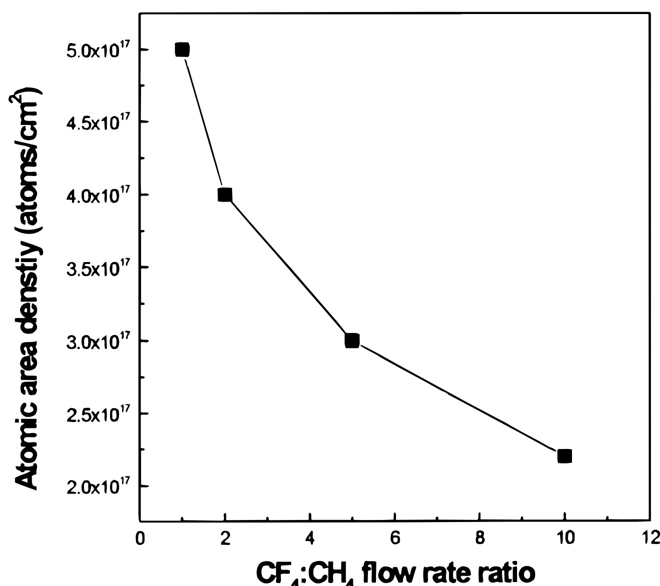

Figure 11. Atomic area density calculated from the ERD-TOF spectra of a-C:F thin films with various CF_4:CH_4 flow-rate ratios.

S0013-4651(98)11-028-5 CCC: $7.00 © The Electrochemical Society, Inc.

is changed slightly. This slight variation of the bonding configuration means insignificant change of the structure of the films, since only substitution of fluorine for hydrogen has occurred. Substitution of a fluorine atom induces the reduction of ionic polarization by the creation of C–F_X bonding in place of C–C or C–H bonding as well as an electronic polarization. However, the ionic polarization does not decrease as much as electronic polarization, since the C–F_2 and C–F_3 bond configurations increase slightly. Therefore, the main reduction mechanism of the dielectric constant in this step is the reduction of the electronic polarization.

Step 2 is a stage in which F content is saturated at 25 atom %, and the C–F_2 and C–F_3 bonding configurations increase, while the C–C (or C–H) and C–F bonding configurations decrease. Total reduction of the dielectric constant is induced by only the reduction of the ionic polarization and the orientation polarization without a change of electronic polarization. As shown in Fig. 6, the ionic polarization and dipole orientation polarization terms in the measured dielectric constant decrease more than the electronic polarization term as the CF_4 flow rate increases. Ionic polarization decreases as the C–F_2 and C–F_3 bonding configuration increases, as disscussed previously.

The orientation polarization of the bond is influenced by the bond dipole moments and the orientation freedom of dipole. Bond dipole moment refers to the degree of the dipole characteristic of the bond, and orientation freedom of the bond dipole is influenced by its neighbors through inductive effects, overlap of electron densities, and the degree of cross-linked structures. The relationship between orientation polarization and the dipole moment is followed as[23]

$$s = \frac{\mu E_d}{3kT} \quad [6]$$

where s is the equilibrium orientation polarization value at which the rate of polarization produced by the field is equal to the rate at which it is destroyed by thermal agitation, μ is the dipole moment, and E_d is the average electric field acting on the dipoles themselves.

In a-C:F films, the reduction of the orientation polarization is observed with increasing C–F_2 and C–F_3 bondings (Fig. 6 and 9), since the bond dipole moment of the molecule is reduced and the orientation of bond dipole is disturbed by the influence of neighboring F atoms. The change of the molecular structure from CH_3F to CHF_3 induces the reduction of the polarization of the C–F bond dipole, since the C–F bond dipole moment decreases. The calculated C–F bond dipole moments in various molecular structures CH_3F, CH_2F_3, and CHF_3 are 1.81, 1.45, and 1.22, respectively.[24] Thus, the change of the molecular structure from CH_3F to CHF_3 reduces the total dipole moments of the molecules from 1.79 to 1.64.[24] The decrease in the dipole moment with changing the bonding configuration results in reduction of the ionic and bond dipolar polarizations, causing the lower dielectric constant.

The movement of the bond dipole from one orientation to another requires enough available energy to overcome the potential energy barrier provided by the neighboring parts of the molecule, electrostatic interactions, or other forms of restraints. As more fluorine atoma are bonded to carbon atoms, the partial charges of the carbon and fluorine ions increase due to a high electronegativity of F atoms, as in Eq. 5. The potential barrier for the orientation movement of dipole with increasing C–F_2 and C–F_3 bonding configuration is larger, since interaction between the bond dipoles in C–F_2 or C–F_3 bonding configurations is larger than that in C–F or C–H configurations. Therefore, the freedom of dipole orientation movement is reduced by the inductive effects of neighboring F ions.

The above-described polarization mechanism can also be expressed in terms of a molecular physical quantity called polarizability, α. The Clausius-Mossotti equation is

$$\alpha = \frac{M}{\rho}\left(\frac{k-1}{k+2}\right)\frac{3\epsilon_0}{N_0} \quad [7]$$

where M is molecular weight, ρ is density, k is the relative dielectric constant, ϵ_0 is the dielectric constant of a vacuum, and N_0 is Avogadro's number. According to Eq. 7, as though the molecules have the same polarizability, the dielectric constants of the films are reduced with the decrease of the density of the film. The density of the film decreases with increasing CF_4:CH_4 flow-rate ratio, since the structure is changed to a less cross-linked structure with a short C–C chain, as discussed in the structural analysis section. Thus, the additional reduction of the dielectric constant of the a-C:F film is induced by decrease of the density of the film due to an increase of CF_4:CH_4 flow-rate ratio.

As a result, the dielectric constant of the a-C:F thin film is reduced by C–F_X bonding configuration as well as the fluorine content, since the ionic and orientation polarization decreases with increasing C–F_2 and C–F_3 bonding configurations.

Conclusion

Fluorinated amorphous carbon thin films as a low dielectric material for ULSI circuits were deposited using remote-type ICP-CVD. Refractive indexes and dielectric constants of the a-C:F films were reduced with increasing CF_4:CH_4 flow rate ratio. However, the composition analyzed by ERD-TOF and AES was not changed significantly with high CF_4:CH_4 flow-rate ratio. The main bonding configuration in the structure of the thin film was changed from C–F bonding to the C–F_2 and C–F_3 bonding as CF_4:CH_4 flow-rate ratio increased. Thus, the atomic area density of the thin films was reduced by producing C–F_2 and C–F_3 bonds, making the structure linear and having a short chain with increasing the CF_4:CH_4 flow-rate ratio. This variation of bonding configuration reduces the ionic and orientation polarization, which is the origin of the decrease in the dielectric constant of the thin films with growing CF_4:CH_4 flow-rate ratio. Therefore, the lower dielectric constant of the amorphous fluorinated carbon thin films can be obtained by creation of C–F_2 or C–F_3 bonding configurations as well as incorporation of fluorine.

Acknowledgment

This work was financially supported by the Ministry of Education through the Interuniversity Semiconductor Research Center (ISRC 97-E-1060) in Seoul National University and by the International Collaborative Research Program of the Ministry of Science and Technology.

Korea Advanced Institute of Science and Technology assisted in meeting the publication costs of this article.

References

1. R. K. Laxman, *Semicond. Int.*, 71 (May 1995).
2. T. Usami, K. Shimigawa, and M. Yoshimaru, *Jpn. J. Appl. Phys.*, **33**, 408 (1994).
3. T. Homma, R. Yamaguchi, and Y. Murao, *J. Electrochem. Soc.*, **140**, 687 (1993).
4. W-T. Tseng, Y-T Hsieh, and C-F Lin, *Solid State Technol.*, **40(2)**, 61 (1997).
5. J-H. Kim, S-H. Seo, S-M. Yun, H-Y. Chang, K-M. Lee, and C-K. Choi, *Appl. Phys. Lett.*, **68**, 1507 (1996).
6. T-M. Lu and J. A. Moore, *MRS Bull.*, **22**(10), 28 (1997).
7. L. A. Sullivan and B. Han, *Solid State Technol.*, **39(5)**, 91 (1996).
8. P. K. Wu, G-R. Yang, J. F. Mcdonald, and T-M. Lu, *J. Electron. Mater.*, **24**, 53 (1995).
9. J. A. Moore, C-I. Lang, T-M. Lu, and G-R. Yang, *Polym. Mater. Sci. Eng.*, **72**, 437 (1995).
10. N. P. Hacker, *MRS Bull.*, **22(10)**, 33 (1997).
11. E. Korczynski, *Solid State Technol.*, **39(4)**, 63 (1996).
12. A. Bubenzer, B. Dischler, G. Brandit, and P. Koidl, *J. Appl. Phys.*, **54**, 4590 (1983).
13. H. Tsai and D. B. Bogy, *J. Vac. Sci. Technol.*, **A5**, 3287 (1987).
14. R. d'Agostino, F. Cramarossa, and F. Illuzzi, *J. Appl. Phys.*, **61**, 2754 (1987).
15. K. Endo and T. Tatsumi, *J. Appl. Phys.*, **78**, 1370 (1995).
16. S. Robles, L. Vaquez, M. Eizenberg, and F. Moghadam, in *Proceedings of the 3rd International Dielectrics for ULSI Multilevel Interconnection Conference, DUMIC*, p. 49, Santa Clara, CA, Feb 10-11, 1997.
17. S. Takehishi, H. Kudo, R. Shinohara, M. Hoshino, S. Fukuyama, J. Yamaguchi, and M. Yamada, *J. Electrochem. Soc.*, **144**, 1797 (1997).
18. S. S. Klein, *Nucl. Instrum. Methods*, **B15**, 464 (1986).
19. S-S. Han, B-H. Jun, K. No, and B-S Bae, *J. Electrochem. Soc.*, **145**, 652 (1998).
20. R. E. Banks, *Organofluorine Chemistry*, p. 58, Plenum Press, New York (1994).
21. H. A. Lorentz, *Ann. Phys.*, **9**, 641 (1880).
22. J. E. Huheey, *Inorganic Chemistry*, p. 262, Harper & Row, New York (1983).
23. C. J. F. Bottcher, O. C. van Belle, P. Bordewijk, and A. Rip, *Theory of Electric Polarization*, 2nd ed., Elsevier, New York (1973).
24. J. W. Smith, *Electric Dipole Moments*, Butterworths, London (1955).